

Influence of a Shield Wire Flashover on the Indirect Lightning Performance Assessment of Distribution Lines

Akifumi Yamanaka and Kazuyuki Ishimoto

Abstract—This paper presents a new aspect of shield wire (SW) modeling for assessing the indirect lightning performance of overhead medium-voltage distribution lines: a flashover (FO) between an SW and the reinforcing bars of a distribution pole or a crossarm (SWFO). In general, an SW is periodically grounded approximately every four to ten poles and not grounded at the other poles. However, owing to lightning-induced overvoltages, the voltage difference between the SW and the distribution pole may even exceed 100 kV, and the SWFO can occur. In this paper, we evaluate the effect of the SWFO on the number of FO occurrences of phase-conductor insulators by the Monte Carlo method using a 2D finite-difference time-domain-based indirect lightning surge analysis program. The effect of the SWFO is more significant in lines with high soil resistivity (a soil resistivity of 1000 Ωm was assumed) regardless of the installation of surge arresters: the total number of FO occurrences markedly differs by up to 50% between cases in which the SWFO is considered and not considered. The analysis presented in this paper will assist the formulation of lightning protection measures particularly, in regions with high-resistivity soils.

Keywords: Medium-voltage distribution line, Lightning-induced outages, Shield wire, Flashover, Monte Carlo method, EMT analysis

I. INTRODUCTION

LIGHTNING is a severe threat to overhead medium-voltage (MV) distribution lines. Since a lightning-induced overvoltage can be generated by an indirect lightning strike, its occurrence frequency is much higher than that of the overvoltage generated by a direct lightning strike to distribution lines. Hence, protection against indirect lightning surges has an important role in reducing the number of temporary or permanent faults. In general, the installation of shield wire(s) (SW), that of surge arrester(s) (SA), and an increased critical flashover (FO) voltage of the insulator are adopted as protection measures [1], [2]. This paper shows a new aspect of SW modeling in assessing the indirect lightning performance of MV distribution lines.

An appropriate design of internal (controllable) parameters, such as the absolute height, the relative position to phase conductors, and the grounding resistance of the SW, is crucial for improving the lightning performance of distribution lines [3], [4]. The grounding spacing of SW is also an internal parameter. The SW is usually periodically grounded approximately every 200–500 m (approximately every four to ten poles). At the other poles, the SW is usually isolated from the distribution pole from the electrical viewpoint. Considering

the above parameters as well as the lightning conditions, the effectiveness of the SW has been studied using various lightning-induced voltage analysis programs, whose results have been validated by theoretical analyses, reduced-scale experiments, and field measurements [5]–[11].

The new aspect of SW modeling introduced in this paper is the FO between an SW isolated from the pole and the reinforcing bars of the distribution pole, hereafter referred to as an SWFO. When an indirect lightning surge enters a distribution line, a large voltage difference that may exceed 100 kV is generated between the SW and the distribution pole. In this case, an FO can occur, the SW is short-circuited to the reinforcing bars of the pole, and, as a result, the pole performs as a down conductor [12]–[14]. Through this phenomenon, the voltages of the phase-conductor insulators are reduced, and, in consequence, the lightning performance can be improved. In other words, the effectiveness of the SW can be greater than that indicated by analyses in literature without considering the SWFO. It is noted that the use of a reinforced concrete pole for supporting distribution lines is assumed. In this paper, we evaluate the effect of the SWFO on the lightning performance by the Monte Carlo (MC) method [15] using an indirect lightning surge analysis program based on the 2D finite-difference time-domain (FDTD) method [16], [17] for the electric field calculation and the Agrawal et al. coupling formula [18] for the induced voltage calculation [19], [20].

The structure of the paper is as follows. Section II presents the line configuration to be studied, the modeling of the line including the SWFO, analysis techniques, and the dependence of the basic characteristics of the insulator voltages on the SW configuration and modeling. Section III presents an evaluation of the indirect lightning performance of distribution lines by the MC method to clarify the effect of the SWFO. Section IV concludes this paper.

II. LINE CONFIGURATION, MODELING, ANALYSIS TECHNIQUES, AND BASIC CHARACTERISTICS

A three-phase overhead distribution line with or without the SW was analyzed by an indirect lightning surge analysis program [19]. In the program, the lightning-induced electric fields were computed by the 2D-FDTD method. Then, using these fields and the Agrawal et al. coupling formula [18], the transient response of a distribution line was computed by electromagnetic transient (EMT) analysis. This section describes EMT analysis models of the distribution line

including the SWFO, analysis techniques, and the basic characteristics of lightning-induced voltages.

A. Line Configuration and Modeling

1) Configuration and Basic Models

Table 1 shows the configuration of the distribution line and modeling. Fig. 1 shows the voltage–current characteristic of the 6.6 kV SA examined in this study. The SW and phase conductors with a length of 2 km were modeled by the Agrawal et al. coupling formula [18]. Both ends of the line were grounded via a multiphase matching circuit. The distribution pole was modeled by a lossless distributed-parameter-line model with a surge impedance of 300 Ω and a traveling wave speed of c_0 (speed of light in free space). The span length was set to 40 m. The grounding of the distribution pole was modeled by the linear resistance R_{gr} given by

$$R_{gr} = \frac{\rho}{2\pi l} \ln \left(1 + \frac{l}{r_{eq}} \right), \quad (1)$$

where ρ is the soil resistivity, and l and r_{eq} are the length and radius of the grounding electrode, respectively [21]. The buried part of the concrete pole was assumed as the electrode, and l and r_{eq} were set to 2 and 0.17 m, respectively. Resistances of 20 and 200 Ω were used for soil resistivities of 100 and 1000 Ωm , respectively.

The FO across the insulator of the phase conductors was modeled using the integral model [22]. In this model, an FO occurs when the time integral D of the insulator voltage exceeds a specific DE value. The integral D is given by

$$D = \int_{t_0}^t [V(t) - V_0]^k dt, \quad (2)$$

where $V(t)$ is the insulator voltage, V_0 is the minimum voltage to be exceeded before the FO process starts, k is a dimensionless

TABLE 1. CONFIGURATION AND MODELING OF A DISTRIBUTION LINE.

Shield wire: Steel wire 22 mm ²	Diameter	6.0 mm
	Height	12.25 m
	Position	0 m
Phase conductors: XLPE insulated copper wire 80 mm ²	Diameter	11.6 mm
	Height	11.5 m
	Position	L1: -0.5 m, L2: 0 m, L3: 0.5 m
Distribution pole	Length	14.0 m
	Diameter	250 mm
	Surge impedance	300 Ω
Length	Span length: 40 m, Total length: 2 km	
Soil resistivity	100, 1000 Ωm	
FO model of insulator	Integral model, $V_0 = 132$ kV, $DE = 66$ kV μs	
FO model of SW-pole gap	FO switch, FO voltage of 50 kV	
Grounding of pole	Linear resistance, 20, 200 Ω	
Grounding of SA	Linear resistance, 30 Ω	

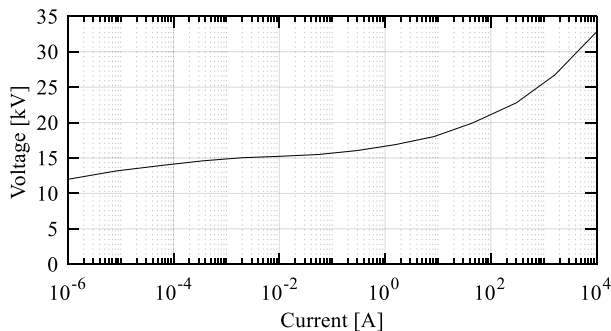


Fig. 1. Voltage–current characteristic of a 6.6 kV SA.

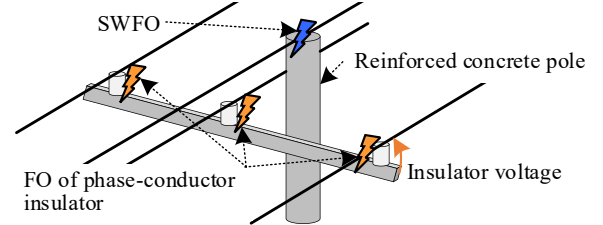


Fig. 2. SWFO and FO of the phase-conductor insulator.

factor, and t_0 is the time at which $V(t)$ exceeds V_0 . k was set to 1. In addition, DE and V_0 were set to the values presented in Table 1, representing a solid-core insulator with a 50% FO voltage of 147 kV and a standard deviation of 4.9 kV [23].

2) FO of SW and Reinforcing Bars of Distribution Pole: SWFO

In addition to the FO of the phase-conductor insulators, the FO between the SW and the reinforcing bars of the distribution pole or metal crossarm (SWFO) was considered. Fig. 2 shows the SWFO and FO of the phase-conductor insulator. Generally, SWs are grounded by a down conductor approximately every 200–500 m (every four to ten poles). At the other poles, the SW is isolated from the distribution pole from the electrical viewpoint; a centimeter-order concrete layer exists between the SW and reinforcing bars inside the pole. Thus, in indirect lightning surge analyses presented in literature, the SW has been grounded approximately every 200–500 m and not grounded at the other points. However, when the induced voltage is generated by indirect lightning, the voltage difference between the SW and the distribution pole can even exceed 100 kV. In this situation, the SW and the reinforcing bars inside the distribution pole can be short-circuited by the FO. In consequence, the distribution pole can perform as a down conductor.

To model the SWFO, we inserted a FO switch operating at 50 kV between the SW and the distribution pole top where the SW was not grounded. Typical concrete poles used in Japan, for instance, have about fifteen main reinforcing bars surrounded by supporting wires, and the distance between the pole surface and the bars or wires is generally about 20 mm. Since the bars and wires are installed uniformly, we can expect that the distance between the pole surface and the bars or wires is almost uniform. In [12], it was shown by an experiment using a test distribution line that the metallic bar inside the concrete pole and a SW is short-circuited by the FO: the FO repeatedly occurred at about 50 kV by a lightning impulse voltage waveform. In [14], it was shown from the observational results and EMT analysis that the FO voltage between the SW and the concrete pole is assumed to be about 60 kV, representing the FO by an ideal switch in the EMT analysis. Thus, the FO between the SW and the pole can be well represented by an ideal switch, and we adopted the FO voltage of 50 kV.

Note that the SWFO may cause a damage to the pole, such as a spark mark or a minor lack of the concrete layer. However, the damage is expected to be not as severe as that caused by the direct lightning hit [24]. To the best of authors' knowledge, the damage due to the SWFO has not caused any problem for the operation of distribution systems (usually the lack of the concrete layer does not cause problems for the operation).

B. Analysis Techniques

1) FDTD Method in 2D Cylindrical Coordinate System

The FDTD method solves time derivative terms of Ampere's and Faraday's laws based on the finite difference. In the 2D-FDTD method, the electromagnetic fields are solved in the 2D cylindrical coordinate system shown in Fig. 3 (a). The radial and vertical electric fields, E_r and E_z , respectively, and the azimuthal magnetic field H_ϕ are allocated in the r - z plane as shown in Fig. 3 (b). For example, the update equation for the magnetic field can be expressed as

$$\begin{aligned} H_\phi^{n+\frac{1}{2}}\left(i+\frac{1}{2}, j+\frac{1}{2}\right) &= H_\phi^{n-\frac{1}{2}}\left(i+\frac{1}{2}, j+\frac{1}{2}\right) \\ &+ \frac{\Delta t/\Delta z}{\mu(i+1/2, j+1/2)} \left\{ E_r^n\left(i+\frac{1}{2}, j+1\right) - E_r^n\left(i+\frac{1}{2}, j\right) \right\} \\ &- \frac{\Delta t/\Delta r}{\mu(i+1/2, j+1/2)} \left\{ E_z^n\left(i+1, j+\frac{1}{2}\right) - E_z^n\left(i, j+\frac{1}{2}\right) \right\}, \end{aligned} \quad (3)$$

where μ is the permeability of the studied medium, Δt is the time step, and Δr and Δz are the cell sizes in the radial and vertical directions, respectively. In the Agrawal et al. coupling formula [18], the horizontal electric field along the overhead line is required. In the analysis program, this electric field was derived from the radial electric field in the 2D-FDTD method by interpolation in the radial [20] and vertical directions, and by considering the direction cosine shown in Fig. 4 as follows:

$$\begin{aligned} E_r(x) &= \alpha_{rr} E_r(i-1/2) + (1-\alpha_{rr}) E_r(i+1/2), \\ \alpha_{rr} &= \frac{x-(i-1/2)\Delta r}{\Delta r}, \end{aligned} \quad (4)$$

$$\begin{aligned} E_r(x, h) &= \alpha_{rz} E_r(x, j-1) + (1-\alpha_{rz}) E_r(x, j), \\ \alpha_{rz} &= \frac{h-(j-1)\Delta z}{\Delta z}, \end{aligned} \quad (5)$$

$$E_x(x, h) = E_r(x, h) \frac{x}{r}. \quad (6)$$

The vertical electric field required in the Agrawal et al. formula [18] was derived in the same manner as the horizontal electric field.

2) Induced Voltage Calculation and EMT Analysis

The Agrawal et al. formula [18] was used to compute the induced voltages. The formula for a single-conductor system is expressed as

$$\begin{aligned} \frac{\partial v^s(x, t)}{\partial x} + L' \frac{\partial i(x, t)}{\partial t} + \int_0^t \xi_g(t-\tau) \frac{\partial i(x, \tau)}{\partial \tau} d\tau \\ = E_x^i(x, h, t), \end{aligned} \quad (7)$$

$$\frac{\partial i(x, t)}{\partial x} + C' \frac{\partial v^s(x, t)}{\partial t} = 0, \quad (8)$$

where v^s and i are the scattered voltage and total current, respectively, and t is time. Moreover, x and h are the horizontal position and height of the line, L' and C' are the per-unit-length inductance and capacitance, and E_x^i and ξ_g are the incident horizontal electric field and transient ground resistance, respectively. Equations (7) and (8) were solved by the second-order FDTD method [25]. The total voltage v was derived from the scattered voltage and the incident voltage given by the

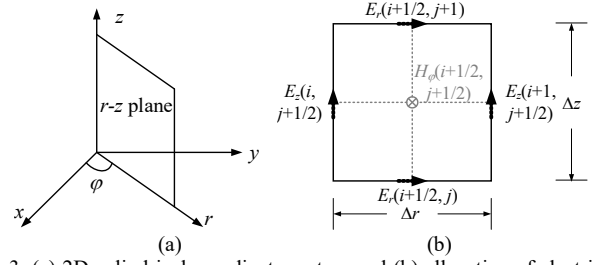


Fig. 3. (a) 2D cylindrical coordinate system and (b) allocation of electric and magnetic fields in the 2D-FDTD method.

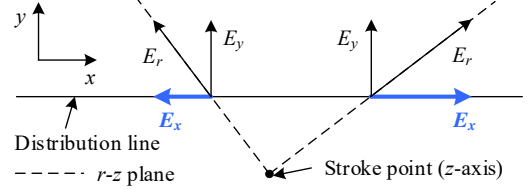


Fig. 4. Conversion of the radial electric field derived in the 2D-FDTD method to the horizontal (x-direction) electric field used in the Agrawal et al. formula [18].

integration of the vertical electric field:

$$v(x, t) = v^s(x, t) + v^i(x, t) = v^s(x, t) - \int_0^h E_z^i(x, z, t) dz. \quad (9)$$

In the analysis program, the integral in (9) was computed following the trapezoidal rule since all the required fields were computed by the FDTD method. The approximate formulae presented in refs. [26], [27] were used to consider the transient ground resistance.

The transient response of the entire system was computed on the basis of EMT analysis with the nodal analysis technique. Circuit elements, such as the distribution pole, grounding resistance, and others, were all transformed into an equivalent conductance and a current source using the trapezoidal technique [28]. The conductance matrix was derived by the sparse tableau approach [29]. A nonlinear element representing the SA was solved using the Newton-Raphson method with a piecewise linear approximation.

The interface between the EMT analysis and the Agrawal et al. formula [18] was modeled using the method presented in [30]. In the method, external fictitious Bergeron lines are considered at both ends of the overhead line with the presence of an exciting LEMP field.

C. Basic Characteristics of Insulator Voltages

The insulator voltages generated in the following four SW configurations were evaluated:

- No SW ("No-SW");
- SW grounded every 200 m (every five poles) and not grounded at other poles (SWFO not considered);
- SW grounded every 200 m (every five poles) and 50 kV FO switch inserted at other poles (SWFO considered);
- SW grounded at every pole.

Note that in cases (b)–(d), a single-phase SW was installed. The comparison between cases (a) and (b)–(d) can reveal the effectiveness of the SW in suppressing induced voltages. Fig. 5 shows the distribution line model. The stroke location was set to $d = 50, 100, 150, 200, 300, 400,$ and 500 m from the center

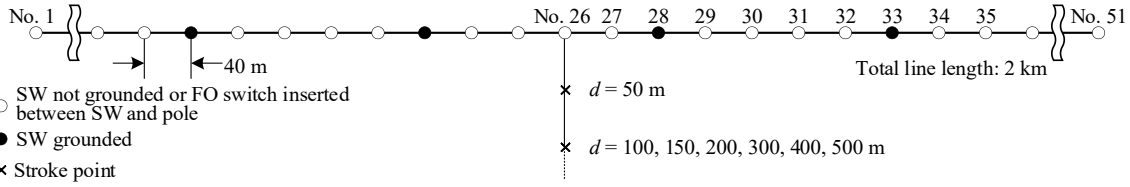


Fig. 5. Distribution line model and SW configuration for discussing the basic characteristics of the lightning-induced insulator voltages.

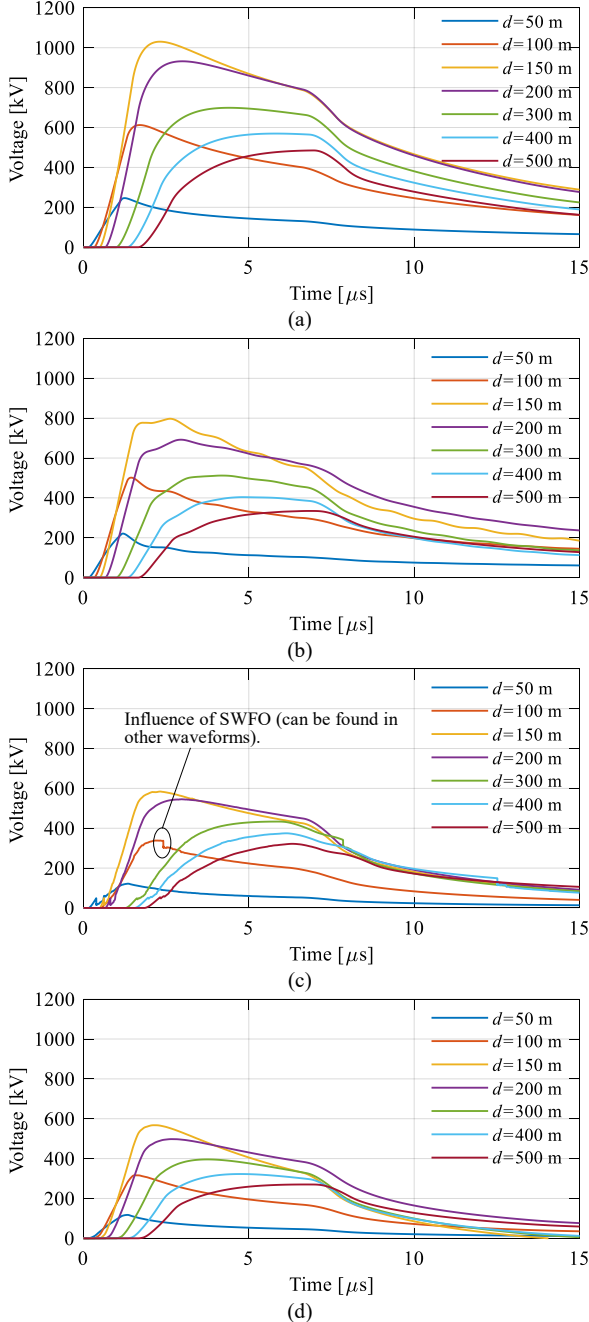


Fig. 6. Insulator voltages generated by indirect lightning for each distance d from the line with soil resistivity of $1000 \Omega\text{m}$ (grounding resistance of 200Ω). The highest insulator voltages are shown. (a) No-SW, (b) SW grounded every 200 m (every five poles), (c) SW grounded every 200 m (every five poles) and SWFO considered at other poles, and (d) SW grounded at every pole.

of the line (pole No.26 in Fig. 5). The lightning was modeled by a transmission line model with a current traveling speed of $100 \text{ m}/\mu\text{s}$ [31]. The current waveform was triangular with a front duration of $1 \mu\text{s}$ and a wavetail time to half value of $70 \mu\text{s}$.

TABLE 2. VOLTAGE PEAKS IN NO-SW CASE*

ρ [Ωm]	Insulator voltage peaks [kV]						
	50	100	150	200	300	400	500
1000	246	612	1030	932	698	570	485
100	173	389	615	531	374	292	242

* ρ : soil resistivity [Ωm]; 50, 100, 150, 200, 300, 400, and 500: distance from line to stroke point [m].

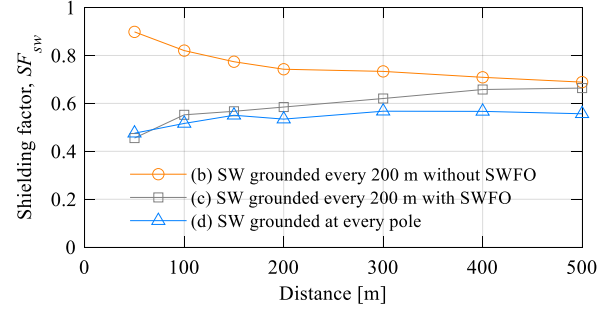


Fig. 7. Shielding factor of phase-to-shield wire voltage, SF_{sw} , derived in cases (b)–(d) for the soil resistivity of $1000 \Omega\text{m}$. The magnitudes of the insulator voltage peaks of the No-SW case are shown in Table 2.

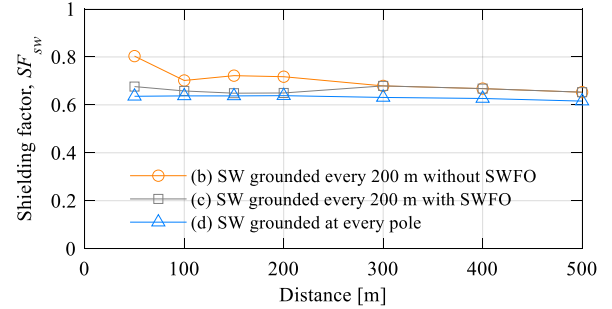


Fig. 8. Same as Fig. 7, but for the soil resistivity of $100 \Omega\text{m}$.

The current peak was set to 20, 80, 180, and 200 kA for $d = 50, 100, 150, \text{ and } 200, 300, 400, 500 \text{ m}$, respectively, following the electro-geometric model (EGM) [32], [33]. These current peaks were used to derive results shown in Fig. 6–Fig. 9 and Table 2. The EGM provides the striking distance r as

$$r = K \times I^b, \quad (10)$$

where I is the current peak and K is a constant determined based on the characteristics of the struck object. In this paper, K was set to 10.0, 9.84, 9.97, and 9.0 for concrete poles, phase conductors, SWs, and ground surface, respectively; b was set to 0.65. These parameters reproduce a field observation result of a direct lightning strike ratio to the pole, phase conductors, and SW [33]. In this analysis, the FO of the phase-conductor insulator was not considered.

The FO between the SW and the reinforcing bars of the distribution pole (SWFO) affects the insulator voltages. Fig. 6 shows the highest insulator voltages generated along the line for the soil resistivity of $1000 \Omega\text{m}$ (a grounding resistance of 200Ω). As expected, the highest insulator voltages were generated

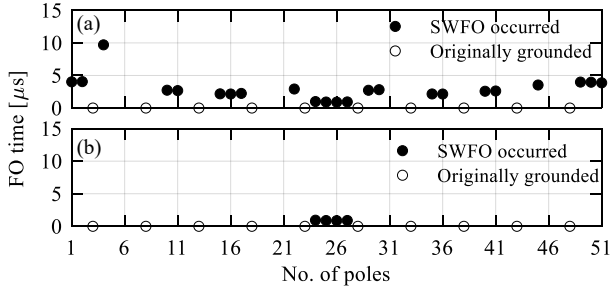


Fig. 9. Occurrences of the SWFO when the distance from the line to the stroke point is 200 m for soil resistivities of (a) 1000 and (b) 100 Ωm .

in the No-SW case, and the lowest insulator voltages were generated when the SW was grounded at every pole. Comparing the insulator voltages in cases (b) and (c), lower insulator voltages are induced in the latter case. This means that the SWFO reduces the lightning-induced voltages.

The characteristics of the insulator voltages are further discussed as follows. Table 2 shows the insulator voltage peaks derived for soil resistivities of 1000 and 100 Ωm , in the No-SW case. Fig. 7 and Fig. 8, respectively, show the shielding factor of the phase-to-shield wire voltage, SF_{sw} [9], for the two soil resistivities, given by:

$$SF_{sw} = \frac{V_{p-sw}}{V'_p} \quad (11)$$

where V_{p-sw} is the phase-to-wire voltage (insulator voltage) induced in the presence of the SW (cases (b)–(d)) and V'_p is the phase-conductor voltage induced in the absence of the SW (case (a)). For both soil resistivities, case (c) provides a lower SF_{sw} than case (b). For the soil resistivity of 1000 Ωm , case (c) provides a lower SF_{sw} than case (b) over the entire distance, while for the soil resistivity of 100 Ωm , SF_{sw} derived for cases (b) and (c) are identical for distances longer than 300 m since no SWFO occurred owing to the lower induced voltages (see Table 2 for voltage peaks V'_p derived in case (a)). Fig. 9 shows the occurrences of the SWFO when the distance from the line to the stroke point was set to 200 m. A larger number of SWFOs occurred for the soil resistivity of 1000 Ωm owing to the higher induced voltages. Thus, it is expected that SWFOs will have a more significant effect on the outage rate for lines with higher soil resistivity (higher grounding resistance).

III. MONTE CARLO SIMULATION FOR ASSESSING INDIRECT LIGHTNING PERFORMANCE OF DISTRIBUTION LINES

A. Analysis Cases

Here, three different SW configurations/models and two different cases of SA installation were analyzed. The SW configurations/models are cases (a)–(c) in Section II.B. The two different cases of SA installation are as follows:

- I. No SAs (“No-SA”);
- II. SAs installed every 400 m.

The MC simulation was performed for six line configurations (cases (I-a)–(I-c) and cases (II-a)–(II-c)) for the first and subsequent strokes. Note that in cases (II-b) and (II-c), the SA was installed at the poles where the SW was grounded. In addition, the SAs were installed for three phases.

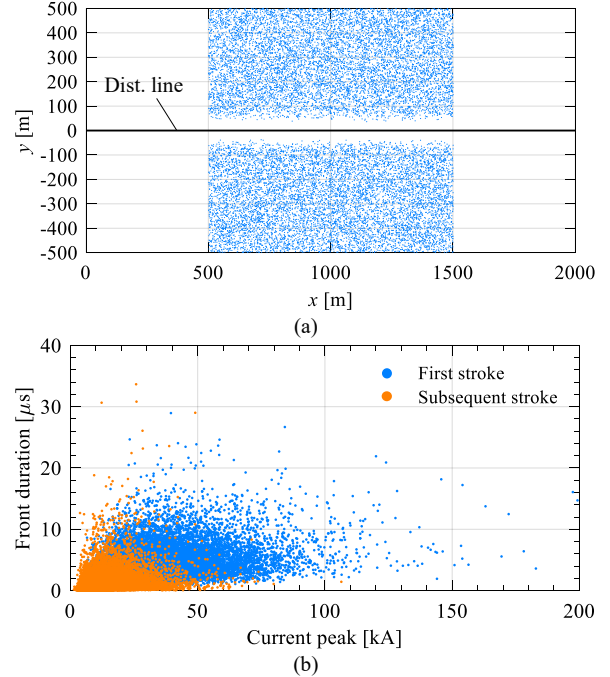


Fig. 10. (a) Stroke location and (b) current properties generated by the MC method in the SW-installed line (indirect events are shown). A correlation between the peak and front duration shown in [34] was considered.

B. Synthesis of Lightning Events and Procedure of the Assessment

The indirect lightning performance of the distribution line was assessed by a total of 20 000 lightning events. First, 20 000 lightning events were randomly generated by the MC method, and current properties of the first stroke are associated with each event considering the log-normal distribution of the peak and front duration with their correlation characterized by the observational results of Berger et al. [34]. Then the EGM was applied to each lightning event, and as a result, in total 17 612 and 17 647 events were classified as indirect lightning in the SW-installed and SW-uninstalled lines, respectively. Finally, current properties of subsequent strokes were associated with each indirect event also considering the log-normal distribution of peak and front duration with their correlation characterized by the observational results of Berger et al. Fig. 10 (a) shows the analyzed 2-km-long line and the stroke location in the SW-installed line, and Fig. 10 (b) shows the current properties of the first and subsequent strokes.

In the MC procedure, the expected annual number of FO occurrences, F_p , is calculated as

$$F_p = \frac{N_{FO}}{N_{tot}} \times A \times N_g, \quad (12)$$

where N_{tot} , N_{FO} , and N_g are the total number of lightning events, the number of FO events, and the annual ground flash density, respectively, and A is the collecting area for the MC procedure; N_{tot} was set to 20 000, A was set to 1 km^2 , and N_g was set to 1 $\text{flash}/\text{km}^2/\text{year}$. In this paper, the number of FO occurrences was separately calculated by the first and subsequent strokes. This approach clarifies whether the SWFO has an influence on the FO occurrences in each stroke or not. Note that for discussing lightning protection measures in actual lines, the FO

occurrences by subsequent strokes should be properly considered: to calculate the annual number of the FO occurrences, the analysis for the subsequent stroke is not required if the corresponding first stroke causes the FO; the number of subsequent strokes per flash should be properly considered.

A triangular current waveform was used in the FO analysis [35]. This waveform provides a conservative assessment of the indirect lightning performance and reduces the computational load. The wavetail time to half value was fixed at $70 \mu\text{s}$ since it has little effect on indirect lightning surges.

C. 2D-FDTD-based Indirect Lightning Surge Analysis Program and MC Procedure: Calculation Time Reduction

The number of electric field calculations required for the indirect lightning surge analysis can be reduced by taking a feature of the indirect lightning surge analysis program with lightning-induced electric field calculation by the 2D-FDTD method into account; the total computation time of MC lightning performance evaluation can be reduced accordingly. Before a large number of indirect lightning surge analyses, for instance, 17 612 and 17 647 times in cases with and without the SW in this paper, respectively, the electric fields were calculated for every rising time of $0.1 \mu\text{s}$ from 0.4 to $29.0 \mu\text{s}$ for the first stroke with an arbitrary current peak (10 kA for example), and they were stored in a memory (287 2D-FDTD calculations were performed). In the 17 612 or 17 647 indirect lightning surge analyses, appropriate electric fields were taken from the memory and used as an input of the Agrawal et al. formula [18] after adjusting the distance, direction, and peak current value. Thus, the number of electric field calculations was reduced by two orders of magnitude; moreover, these calculated electric fields can be used to analyze any line configuration.

D. Results and Discussion

The SWFO has an impact on the number of FO occurrences, especially for the higher soil resistivity (higher grounding resistance). Fig. 11 shows the annual number of FO occurrences per 100 km of the line evaluated by the MC method in the SA-uninstalled cases (cases (I-a)–(I-c)). The numbers of FO occurrences in cases (I-b) and (I-c) markedly differ by 30–40%, particularly for the soil resistivity of $1000 \Omega\text{m}$, as expected from the discussion on the basic characteristics of insulator voltages in Section II.B. The effectiveness of the SW may have been underestimated in literature, especially for high-soil-resistivity conditions. The number of two- and three-phase FO (2,3FO) occurrences in case (I-c) is less than half of that in case (I-b) for the soil resistivity of $1000 \Omega\text{m}$. This means that the installation of an SW can significantly suppress lightning-induced outages in an ungrounded neutral system.

The SWFO also has an impact on the FO occurrence in the SA-installed line. Fig. 12 shows the number of FO occurrences in the SA-installed cases (cases (II-a)–(II-c)). The numbers of FO occurrences in cases (II-b) and (II-c) are highly different, particularly for the soil resistivity of $1000 \Omega\text{m}$. The SWFO at the SA-uninstalled poles, which becomes additional grounding points, helps to distribute the effect of the SA, thus suppressing

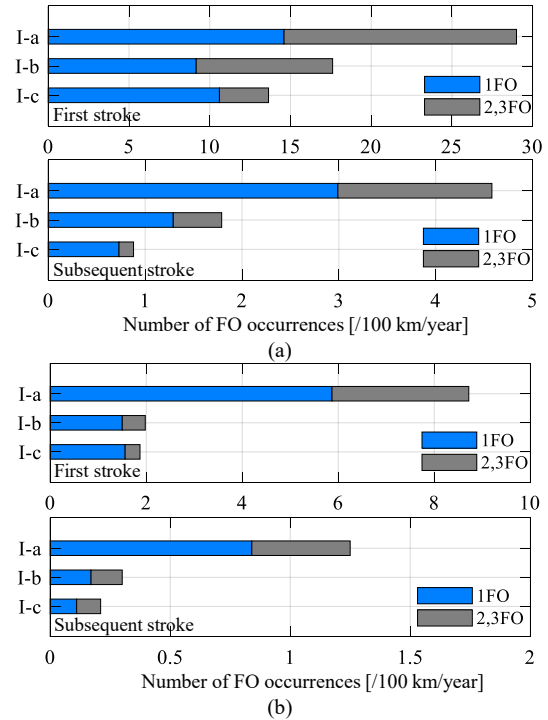


Fig. 11. FO occurrence in (I-a) No-SW, (I-b) SW grounded every 200 m, and (I-c) SW grounded every 200 m and SWFO considered for soil resistivities of (a) 1000 and (b) 100 Ωm . “1FO” denotes a single-phase FO occurrence, and “2, 3FO” denotes two- and three-phase FO occurrences, respectively.

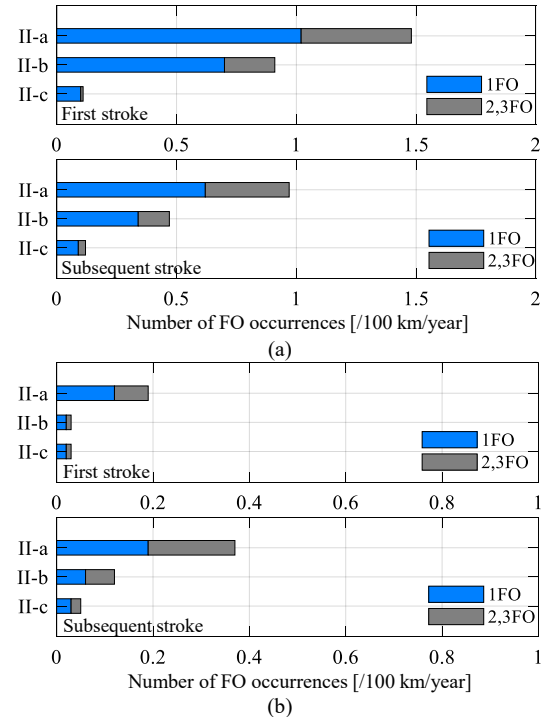


Fig. 12. Same as Fig. 11, but the SA was installed every 400 m (every ten poles).

the insulator voltage. Note that for the soil resistivity of 100 Ωm , the number of FO occurrences is higher in the subsequent stroke than in the first stroke. This is because the FO occurrence is more sensitive to the wavefront duration than the current peak in the SA-installed line [7]. When the SA interval was set to 200 m, the number of FO occurrences is also higher in the subsequent stroke than in the first stroke for the soil resistivity

of 1000 Ωm , although this is not shown since the number of FO occurrences is almost zero.

The above results and discussion suggest that the SWFO has a significant impact on the number of FO occurrences in both SA-installed and SA-uninstalled lines, especially in lines with high soil resistivity (high grounding resistance).

IV. CONCLUSIONS

This paper presented a new aspect of SW modeling for evaluating the indirect lightning performance of overhead MV distribution lines: an FO between an SW and the reinforcing bars of a distribution pole (SWFO) at the poles where the SW is kept not grounded. The SWFO reduces the phase-conductor insulator voltages, especially in lines with high soil resistivity (high grounding resistance). Accordingly, the number of FO occurrences evaluated by the MC method is markedly different in cases with the SWFO considered and not considered: the total numbers of FO and 2,3FO occurrences are reduced by 30–40% and more than 50%, respectively, in SA-uninstalled lines, and the reduction is even greater in SA-installed lines. The analysis will assist the formulation of lightning protection measures, especially in regions with high soil resistivity.

V. REFERENCES

- [1] *IEEE guide for improving the lightning performance of power overhead distribution lines*, IEEE Std. 1410-2010, Jan. 2011.
- [2] Subcommittee for Power Distribution Systems, Lightning Protection Design Committee, "Guide for lightning protection design for power distribution lines," *CRIEPI Rep.*, no. T69, 2002 (in Japanese).
- [3] A. Andreotti et al., "On the role of shield wires in mitigating lightning-induced overvoltages in overhead lines - Part I: a critical review and a new analysis," *IEEE Trans. Power Del.*, vol. 38, no. 1, pp. 335–344, Feb. 2023.
- [4] A. Andreotti et al., "On the role of shield wires in mitigating lightning-induced overvoltages in overhead lines - Part II: simulation results for practical configurations," *IEEE Trans. Power Del.*, vol. 38, no. 1, pp. 345–352, Feb. 2023.
- [5] S. Yokoyama, "Calculation of lightning-induced voltages on overhead multiconductor systems," *IEEE Trans. Power Appar. Syst.*, vol. PAS-103, no. 1, pp. 100–108, Jan. 1984.
- [6] M. Paolone, C. A. Nucci, E. Petrache, and F. Rachidi, "Mitigation of lightning-induced overvoltages in medium voltage distribution lines by means of periodical grounding of shielding wires and of surge arresters: modeling and experimental validation," *IEEE Trans. Power Del.*, vol. 19, no. 1, pp. 423–431, Jan. 2004.
- [7] K. Michishita, M. Ishii, and Y. Hongo, "Flashover rate of distribution line due to indirect negative lightning return strokes," *IEEE Trans. Power Del.*, vol. 24, no. 1, pp. 472–479, Jan. 2009.
- [8] F. H. Silveira, A. De Conti, and S. Visacro, "Voltages induced in single-phase overhead lines by first and subsequent negative lightning strokes: influence of the periodically grounded neutral conductor and the ground resistivity," *IEEE Trans. Electromagn. Compat.*, vol. 53, no. 2, pp. 414–420, May 2011.
- [9] A. Piantini, "Lightning-induced voltages on distribution lines with shield wires," *2016 33rd Int. Conf. on Lightning Protection (ICLP)*, Estoril, Portugal, Sep. 2016, pp. 1–5.
- [10] M. Brignone, D. Mestriner, R. Procopio, A. Piantini, and F. Rachidi, "Evaluation of the mitigation effect of the shield wires on lightning induced overvoltages in MV distribution systems using statistical analysis," *IEEE Trans. Electromagn. Compat.*, vol. 60, no. 5, pp. 1400–1408, Oct. 2018.
- [11] A. Piantini, "Analysis of the effectiveness of shield wires in mitigating lightning-induced voltages on power distribution lines," *Electr. Power Syst. Res.*, vol. 159, pp. 9–16, Jun. 2018.
- [12] A. Asakawa, "Experimental study of overvoltages and flowing currents according to grounding methods of the pole installed transformer on power distribution lines," *CRIEPI Rep.*, no. H04007, Jun. 2005 (in Japanese).
- [13] A. Takahashi, T. Hidaka, K. Ishimoto, and A. Asakawa, "Influence of grounding resistance connecting to surge arresters on effectiveness of lightning protection caused by direct hit for power distribution lines," *IEEEJ Trans. Power and Energy*, vol. 131, no. 5, pp. 472–480, May 2011 (in Japanese).
- [14] T. Miyazaki, S. Okabe, and S. Sekioka, "An experimental validation of lightning performance in distribution lines," *IEEE Trans. Power Del.*, vol. 23, no. 4, pp. 2182–2190, Oct. 2008.
- [15] A. Borghetti, C. A. Nucci, and M. Paolone, "An improved procedure for the assessment of overhead line indirect lightning performance and its comparison with the IEEE Std. 1410 method," *IEEE Trans. Power Del.*, vol. 22, no. 1, pp. 684–692, Jan. 2007.
- [16] K. Yee, "Numerical solution of initial boundary value problems involving Maxwell's equations in isotropic media," *IEEE Trans. Antennas Propagat.*, vol. 14, no. 3, pp. 302–307, May 1966.
- [17] Y. Baba and V. A. Rakov, "Finite-difference time-domain method," in "Lightning-induced effects in electrical and telecommunication systems," pp. 83–128, IET, London, UK, 2020.
- [18] A. K. Agrawal, H. J. Price, and S. H. Gurbaxani, "Transient response of multiconductor transmission lines excited by a nonuniform electromagnetic field," *IEEE Trans. Electromagn. Compat.*, vol. 22, no. 2, pp. 119–129, May 1980.
- [19] A. Yamanaka and K. Ishimoto, "Revisiting the indirect lightning performance of distribution lines: flashover analysis of typical Japanese lines by the Monte Carlo method," *13th Int. Workshop on High Volt. Eng. (IWHV 2022)*, No. EPP-22-119, SP-22-054, HV-22-100, Nov. 2022.
- [20] H.-M. Ren et al., "Analysis of lightning-induced voltages on overhead lines using a 2-D FDTD method and Agrawal coupling model," *IEEE Trans. Electromagn. Compat.*, vol. 50, no. 3, pp. 651–659, Aug. 2008.
- [21] A. C. Liew and M. Darveniza, "Dynamic model of impulse characteristics of concentrated earths," *Proc. IEE*, vol. 121, no. 2, pp. 123–135, Feb. 1974.
- [22] M. Darveniza, "The generalized integration method for predicting impulse volt-time characteristics for non-standard wave shapes – a theoretical basis," *IEEE Trans. Electr. Insul.*, vol. 23, no. 3, pp. 373–381, Jun. 1988.
- [23] K. Ishimoto, F. Tossani, F. Napolitano, A. Borghetti, and C. A. Nucci, "Direct lightning performance of distribution lines with shield wire considering LEMP effect," *IEEE Trans. Power Del.*, vol. 37, no. 1, pp. 76–84, Feb. 2022.
- [24] S. Yokoyama, T. Sato, and A. Takahashi, "Practical lightning protection design for overhead power distribution lines," *2014 Int. Conf. on Lightning Protection (ICLP)*, Shanghai, China, Oct. 2014, pp. 789–795.
- [25] M. Paolone, C. A. Nucci, and F. Rachid, "A new finite difference time domain scheme for the evaluation of lightning induced overvoltages on multiconductor overhead lines," *Proc. Int. Conf. Power Syst. Transients*, no. 01IPST103, pp. 1–7, Rio de Janeiro, Brazil, 2001.
- [26] E. D. Sunde, *Earth conduction effects in transmission systems*. New York, NY, USA: Van Nostrand, 1968.
- [27] F. Rachidi, C. A. Nucci, and M. Ianoz, "Transient analysis of multiconductor lines above a lossy ground," *IEEE Trans. Power Del.*, vol. 14, no. 1, pp. 294–302, Jan. 1999.
- [28] H. Dommel, "Digital computer solution of electromagnetic transients in single-and multiphase networks," *IEEE Trans. Power Appar. Syst.*, vol. PAS-88, no. 4, pp. 388–399, Apr. 1969.
- [29] G. Hachtel, R. Brayton, and F. Gustavson, "The sparse tableau approach to network analysis and design," *IEEE Trans. Circuit Theory*, vol. 18, no. 1, pp. 101–113, 1971.
- [30] F. Napolitano et al., "An advanced interface between the LIOV code and the EMTP-RV," *Proc. 2008 29th Int. Conf. Lightning Protection (ICLP)*, no. 6b-6-1, pp. 1–12, Uppsala, Sweden, Jun. 2008.
- [31] Y. Baba and V. A. Rakov, "On the transmission line model for lightning return stroke representation," *Geophys. Res. Lett.*, vol. 30, no. 24, Dec. 2003.
- [32] H. R. Armstrong and E. R. Whitehead, "Field and analytical studies of transmission line shielding," *IEEE Trans. Power Appar. Syst.*, vol. PAS-87, no. 1, pp. 270–281, Jan. 1968.
- [33] K. Ishimoto, "Assessment program of direct lightning performance for medium voltage distribution lines: —evaluation of flashover and surge arrester absorption energy—," *IEEEJ Trans. Power and Energy*, vol. 142, no. 2, pp. 98–105, Feb. 2022 (in Japanese).
- [34] K. Berger, R. B. Anderson, and H. Kroeninger, "Parameters of lightning flashes," *Electra*, no. 41, pp. 23–37, 1975.
- [35] A. Borghetti, F. Napolitano, C. A. Nucci, and F. Tossani, "Influence of the return stroke current waveform on the lightning performance of distribution lines," *IEEE Trans. Power Del.*, vol. 32, no. 4, pp. 1800–1808, Aug. 2017.